Highly Substituted Azulene Dyes as Multifunctional NLO and Electron-Transfer Compounds

Christoph Lambert,*[a] Gilbert Nöll,[a] Manfred Zabel,[b] Frank Hampel,[c] Elmar Schmälzlin,[d] Christoph Bräuchle,[d] and Klaus Meerholz[d, e]

Dedicated to the memory of PD Dr. J. Jens Wolff (1961 – 2001)

Abstract: Two highly substituted azulene derivatives were synthesised by Pd-mediated dimerisation from the corresponding tolan species. One azulene derivative (**2**) has donor functionalities (dianisylaminophenyl and dianisylamino) in the 1-, 2-, 3- and 6-positions, while the other (**1**) has donors (dianisylaminophenyl) in the 2- and 6-positions and acceptors (nitrophenyl) in the 1- and 3-positions. Each azulene derivative shows strong bond length alternation in the solid state, determined by X-ray crystal analysis, and an intense CT band around 450 – 500 nm in its UV/Vis spectrum. The first-order hyperpolarisability of **1** and of **2** was measured by hyper-Rayleigh scattering and is about that of disperse red DR1. Both azulene derivatives show multiple oxidation processes. The intramolecular adiabatic ET behaviour of the mixed valence radical cations of **1** and of **2** was investigated by UV/Vis/NIR spectroelectrochemistry. The intervalence-CT band of $\mathbf{1}^+$ could be analysed by the Generalised Mulliken – Hush theory, which yields an electronic coupling $V = 1140\ \mathrm{cm}^{-1}$ for the optically induced adiabatic hole transfer.

Keywords: azulene · electron transfer · hyperpolarisability · mixed-valent compounds · triarylamines

Introduction

Azulene and its derivatives have been thoroughly investigated, due to their unusual photophysical behaviour, such as their dipolar character, their long wavelength absorption and the violation of Kasha's rule. Owing to these features, azulene has been incorporated into a number of organic materials, such as electrically conducting polymers,[1, 2] charge-transfer salts,[3] molecular switches[4] and chromophores with nonlinear optical (NLO) properties.[5–11] In most of these last systems, azulene as the parent chromophore is monosubstituted and either its electron-rich five-membered ring serves as an electron donor combined with an acceptor or its electron-deficient seven-membered ring serves as an electron acceptor combined with a donor through a π-bridging system. In only one of these cases[9] does azulene itself act as a π-bridge substituted by an acceptor and a donor. In this paper we report the (non)linear optical and electron-transfer properties of two azulene derivatives: one substituted by two donor groups along the azulene axis and two acceptor groups in lateral positions (**1**) and another substituted by three triarylamine and one dianisylamino donor groups (**2**).

Owing to the intrinsic push – pull character of the central azulene moieties, the chromophores **1** and **2** are expected to display second-order nonlinear optical (NLO) properties, which were investigated by hyper-Rayleigh scattering (HRS).[12] Because of the reversibly oxidisable character of the triarylamine moieties, the azulene derivatives also show intramolecular electron-transfer processes in partially oxidised (mixed valence, MV) states.[13, 14]

The standard NLO chromophore is a one-dimensional π-system substituted by a donor and an acceptor group at either

[a] Prof. Dr. C. Lambert, Dr. G. Nöll
Institut für Organische Chemie
Bayerische Julius-Maximilians-Universität Würzburg
Am Hubland, 97074 Würzburg (Germany)
Fax: (+49) 931-888-4606
E-mail: lambert@chemie.uni-wuerzburg.de

[b] Dr. M. Zabel
Naturwissenschaftliche Fakultät IV
Chemie und Pharmazie, Zentrale Analytik
Universität Regensburg
93040 Regenburg (Germany)

[c] Dr. F. Hampel
Institut für Organische Chemie
Friedrich-Alexander-Universität Erlangen-Nürnberg
Henkestrasse 42, 91054 Erlangen (Germany)

[d] Dr. E. Schmälzlin, Prof. Dr. C. Bräuchle, Prof. Dr. K. Meerholz
Department Chemie
Ludwig-Maximilians-Universität München
Butenandtstrasse 11, 81377 München (Germany)

[e] Prof. Dr. K. Meerholz
Institut für Physikalische Chemie
Universität zu Köln
Luxemburgerstrasse 116, 50939 Köln (Germany)

DOI: 10.1002/chem.200304923

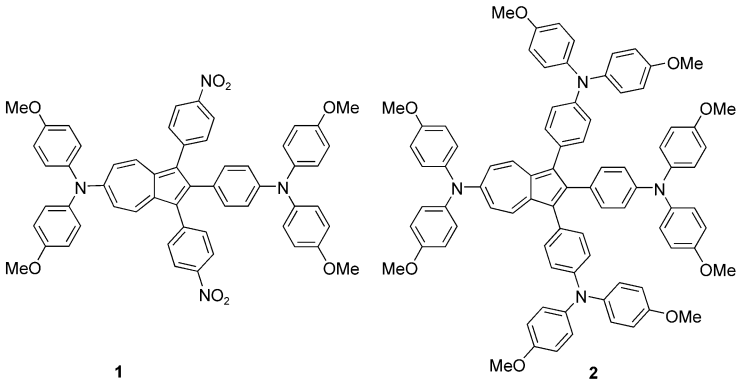

end.[15, 16] Thanks to these substituents, the chromophore shows a charge-transfer (CT) absorption in the UV/Vis, associated with a large difference in the ground state and the excited state dipole moments. According to Oudar and Chemla,[17] the first-order hyperpolarisability β_{zzz} of such a chromophore can be estimated by the two-level approach [Eq. (1)]:

$$\beta_{zzz}^{2\omega} = \frac{1}{\hbar^2}\frac{(\mu_e - \mu_g)\mu_{eg}^2}{\omega_{eg}^2}\frac{\omega_{eg}^4}{(\omega_{eg}^2 - 4\omega^2)(\omega_{eg}^2 - \omega^2)} \quad (1)$$

where μ_{eg} is the transition moment between the ground state and the first excited singlet state (which can be obtained from band integration), $\mu_e - \mu_g$ is the dipole moment difference between the ground and excited CT state, and ω_{eg} and ω are the energy of the CT transition and of the incident laser beam used for the HRS measurement, respectively. In recent years, multidimensional, so-called "octupolar" chromophores, in which more than one CT transition is involved, have attracted considerable interest both because of possibly enhanced first-order hyperpolarisabilities relative to one-dimensional analogues and because of the increased chances of obtaining single crystals with acentric space groups, a prerequisite for observation of second-order NLO phenomena in the crystalline state.[18, 19] In these cases, multi-state equations have to be used for a first-order description of the hyperpolarisability.[20, 21]

Many of the chromophores used for NLO investigations also exhibit interesting electron-transfer behaviour.[22] Basic aspects of electron-transfer (ET) theory have been investigated by use of one-dimensional compounds in which two redox centres are connected by a conjugate or nonconjugate bridge.[13, 14] If the two redox centres have different redox states, an electron or a hole can be transferred by optical or thermal excitation. In most cases, the redox centres are ligand coordinate metal centres,[23–25] but a number of purely organic mixed valence species are also known, among them bis(hydrazine) compounds,[26, 27] bis(quinone) compounds[28, 29] and pentakis(thiophenyl)benzene species,[30] as well as bis(triarylamine) species.[22, 31–35] These last compounds are widely used as hole-transport components[36] in optoelectronic devices such as photorefractive materials, photoconductors, photovoltaic cells, and so deserve special attention.[37–39]

We recently investigated a series of linear bis(triarylamine) radical cations in which two states (hole located on the one triarylamine and hole located on the other) are degenerate in energy,[33–35] together with multidimensional species in which four or six triarylamine redox centres are present[40, 41] and polymers.[42]

The electronic situation of a one-dimensional ET system such as $\mathbf{1}^+$ can be described by mixing two diabatic (noninteracting) states in the secular determinant Equation (2).[43–46] In this equation, quadratic potentials depending on the ET coordinate x are used for the two diabatic states, λ_1 and λ_2 represent the Marcus reorganisation energies, which are assumed to be equal for both states as an approximation, and the coupling is given by V. The resulting potential energy diagram is shown in Figure 1.

$$\begin{vmatrix} \lambda_1 x^2 - \varepsilon & V \\ V & \lambda_2(1-x)^2 + \Delta G^0 - \varepsilon \end{vmatrix} = 0 \quad (2)$$

Because of the different substituents attached to the aryl units in, say, $\mathbf{TD}^+$ (see Figure 1), the state in which the hole is localised at the right-hand triarylamine unit is more stable than the one in which the hole is localised at the left-hand triarylamine group. It is therefore possible to lift one local triarylamine redox potential and thus to introduce a free energy difference ΔG^0 between the two states described above.[47–49]

The coupling of the two diabatic states (dashed line in Figure 1) yields two adiabatic states (solid lines in Figure 1). Optical excitation from the minimum of the double well potential to the excited state causes a hole to be transferred from one triarylamine to the other. This optical excitation at $\tilde{\nu}_{max}$ is usually seen in the NIR and is termed an intervalence charge-transfer band (IV-CT). From Figure 1 it is obvious that $\tilde{\nu}_{max}$ consists of the reorganisation energy λ and the free energy difference ΔG^0. Application of the Generalised Mulliken–Hush analysis [Eq. (3)] to this band yields the electronic coupling V.[44, 45, 50] In Equation (3), μ_{eg} is the transition moment of the IV-CT band, and $\Delta\mu_{ab}$ is the diabatic dipole moment difference, approximated by the geometric N–N distance, $\Delta\mu_{ab} = e \times r$.[51]

$$V = \frac{\mu_{eg}\tilde{\nu}_{max}}{\Delta\mu_{ab}} \quad (3)$$

In these azulene radical cations, the free energy difference ΔG^0 is mainly introduced by the asymmetry of the 2-phenylazulene moiety itself and to some degree by the substituents in lateral positions. While $\mathbf{1}^+$ behaves as a one-dimensional ET system, there are three mixed-valence radical cations in $\mathbf{2}$: $\mathbf{2}^+$, $\mathbf{2}^{2+}$ and $\mathbf{2}^{3+}$, owing to the presence of the four triarylamine redox centres. All these radical cations potentially display multidimensional ET pathways.[40, 41, 52] At this point we should mention that we were unfortunately not successful in analysing these multidimensional ET pathways in the case of **2**.

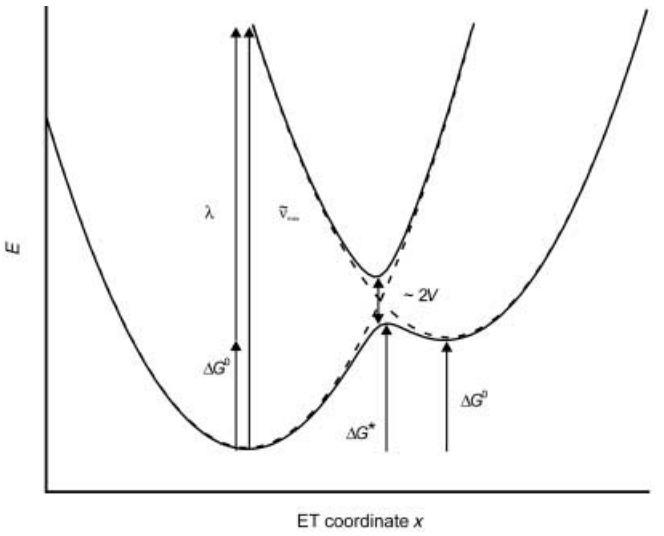

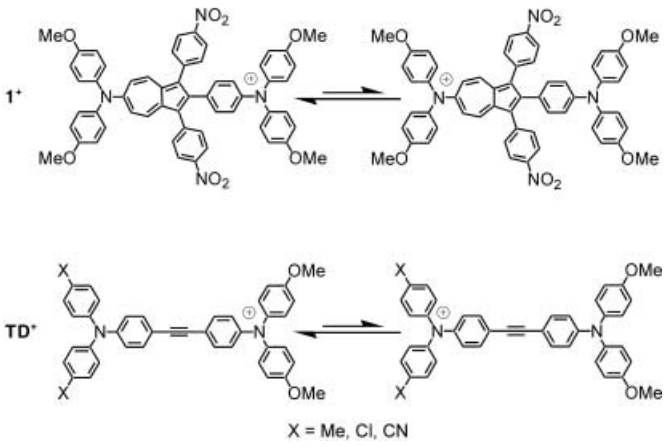

Figure 1. Potential energy diagram for the intramolecular ET processes of $\mathbf{1}^+$ and of $\mathbf{TD}^+$. The adiabatic potentials (solid lines) were constructed from the diabatic potentials (dashed lines) and Equation (2).

Results and Discussion

Synthesis: While treatment of *N,N,N′,N′*-tetraanisyltolandiamine **TATD** with catalytic amounts of $[Co_2(CO)_8]$ gives the corresponding hexaarylbenzene species,[41] the reaction with Pd^{II} salts yields the azulene derivatives.[41, 53, 54] The syntheses of **1** and **2** were therefore achieved by Pd-mediated coupling of the correspondingly substituted tolans according to Scheme 1. Stoichiometric amounts of $[Pd(PhCN)_2Cl_2]$ (one equivalent per mol tolan) were necessary to convert the tolans into the azulenes in low yields. Attempts to run the reaction with catalytic amounts of Pd salt failed. Similar problems were reported by Müller and Zountsas[53, 54] who were the first to report Pd-mediated coupling of tolans to azulenes. In our case the main problem of the conversion of the tolans into the azulenes is the sensitivity of the azulene solutions towards air, which is even higher in the presence of silica gel, resulting in decomposition during purification by chromatography. Conversion of tolans into azulenes by Lewis acids have been reported in the literature,[55] but this was not followed in this work because of the general sensitivity of our triarylamine species towards acids.

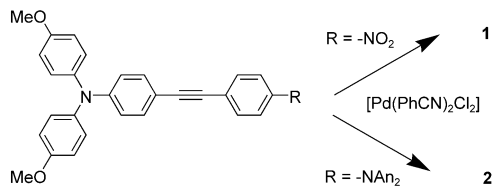

Scheme 1. Synthetic routes to **1** and **2**.

X-ray structure analysis: The molecular structures of **1**·EtOAc and of **2**·MeCN have been investigated by X-ray crystal analysis (see Figure 2). Crystal data and data collection information can be found in Table 1, while selected distances and angles are collected in Table 2.

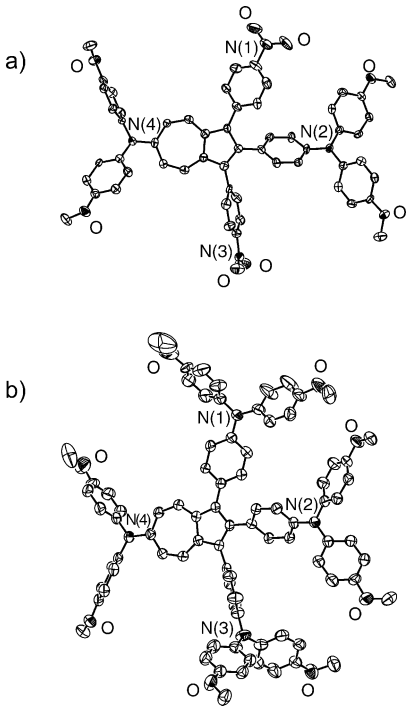

Figure 2. ORTEP plots of the molecular structures of a) **1**·EtOAc and b) **2**·MeCN in the crystalline state. The solvent molecules incorporated in the crystals are omitted for clarity.

Despite the different substituents, the azulene moieties of both derivatives show essentially the same C···C bond lengthss, as well as the same dihedral angles of the phenyl substituents. The most remarkable feature is the asymmetry of the azulene group found in both derivatives **1** and **2**. The azulene systems show significant bond length alternation, which results in a strong deviation from local C_{2v} symmetry; the azulene moiety has local C_s symmetry. In addition, one of the phenyl substituents attached to the 1-position is significantly more twisted out of the azulene plane than the one attached to the 3-position. Although the precise structure of unsubstituted azulene is not known, due to disorder in the crystal,[56] computational studies indicate a very shallow ground-state potential energy surface where the C_{2v} and C_s

Table 1. Crystal data and data collection information.

	1·EtOAc	**2**·MeCN
diffractometer	Nonius diffractometer with CCD	STOE-IPDS
empirical formula	$C_{60}H_{52}N_4O_{10}$	$C_{86}H_{75}N_5O_8$
formula weight	989.09	1296.57
T [K]	173(2)	173(1)
λ [Å]	0.71073	0.71073
crystal system	triclinic	triclinic
space group	$P\bar{1}$	$P\bar{1}$
unit cell dimensions		
a [Å]	9.1109(18)	13.3412(13)
b [Å]	13.251(3)	15.4426(14)
c [Å]	21.448(4)	17.4175(14)
α [°]	94.73(3)	101.334(10)
β [°]	91.49(3)	90.980(11)
γ [°]	104.01(3)	101.653(11)
V [Å^3]	2501.0(9)	3439.9(6)
Z	2	2
ρ_{calcd} [Mg m^{-3}]	1.313	1.233
absorption correction	numeric	none
absorption coefficient [mm^{-1}]	0.090	0.08
F(000)	1040	1349
crystal size [mm^3]	0.30 × 0.30 × 0.30	0.22 × 0.18 × 0.18
θ range for data collection [°]	2.54 to 23.73	1.85 to 25.22
index ranges	$-10 \le h \le 9$ $-14 \le k \le 14$ $0 \le l \le 24$	$-15 \le h \le 15$ $-18 \le k \le 18$ $-20 \le l \le 20$
refls collected	7783	27163
independent refls	7560 [R(int) = 0.0643]	11567 [R(int) = 0.0776]
refinement method	full-matrix least-squares on F^2	full-matrix least-squares on F^2
data/restraints/parameters	7560/0/667	11567/0/887
GoF on F^2	1.022	0.772
final R indices [$I > 2\sigma(I)$]		
$R1$	0.0737	0.0587
$wR2$	0.1574	0.1191
R indices (all data)		
$R1$	0.2374	0.1672
$wR2$	0.2339	0.1500
largest diff. peak and hole [e Å^{-3}]	1.072 and −0.598	0.761 and −0.340

minima are quite close in energy.[57] Thus, small perturbations such as the presence of substituents might easily distort an otherwise more stable C_{2v} geometry towards a C_s geometry, as found in our cases and in the recently described X-ray structure analysis of the cycloaddition product of azulene and furan[58] and in the complex of 1,3,5-trinitrobenzene and azulene.[59] Whether the observed strong bond length alternation is also present in solution and whether it has an effect on the optical properties remains to be elucidated.

In **2**, the trigonal coordination sphere at the nitrogen centre N4 is planar (angle sum 359.9°) while those at N1 (357.9°), N2 (358.9°) and N3 (358.5°) are slightly pyramidal. This emphasises stronger π-conjugation of the N4 lone pair with the electron-deficient seven-membered ring system. In **1** the N4 angle sum is again 360.0° but that at N2—at 359.9°—also indicates stronger π-overlap.

While the triarylamine groups around N2 and N4 in **1** and around N1, N2 and N4 in **2** are coplanar with the azulene units, the one around N3 in **2** is not but is turned out of the azulene plane, presumably in order to avoid steric crowding.

Table 2. Selected bond lengths [Å] and dihedral angles [°].

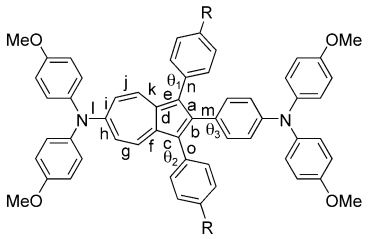

	1	**2**
a	1.430(9)	1.440(5)
b	1.392(9)	1.403(5)
c	1.411(9)	1.417(5)
d	1.470(9)	1.456(5)
e	1.425(9)	1.416(5)
f	1.395(9)	1.402(6)
g	1.369(9)	1.369(6)
h	1.413(9)	1.409(6)
i	1.412(8)	1.399(5)
j	1.379(8)	1.388(5)
k	1.392(9)	1.401(5)
l	1.399(8)	1.397(5)
m	1.474(9)	1.471(6)
n	1.465(9)	1.476(5)
o	1.466(9)	1.483(5)
θ1	41	39
θ2	59	64
θ3	49	43

Linear and nonlinear optical properties: The UV/Vis spectra of **1** and of **2** were recorded in several solvents (see Figure 3 and Table 3). Each azulene derivative shows a very intense absorption between 450–480 nm. We tentatively assign this to an intramolecular CT band because of its band shape,

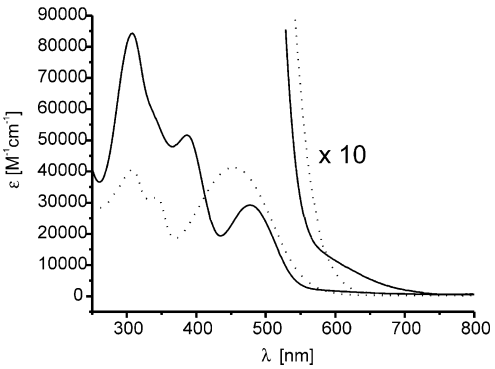

Figure 3. UV/Vis spectra of **1** (dotted line) and of **2** (solid line) in CH_2Cl_2.

Table 3. Absorption data of the longest-wavelength band.

	λ_{max}(Et_2O) [nm]	$\lambda_{max}/\varepsilon$ (CH_2Cl_2) [nm]/[M^{-1}cm^{-1}]	λ_{max}($CHCl_3$) [nm]	λ_{max}(THF) [nm]	λ_{max}(MeCN) [nm]	λ_{max}(DMSO) [nm]
1	441	453/43800	458	449		447
2	475	475/28600	480	477	466	471

although it is not obvious which molecular unit plays the donor and which the acceptor in this excitation. Preliminary AM1-CI computations for **1** suggest a mixing of three contributions: a CT excitation within the azulene moiety and between the five-membered ring (donor) with the nitrophenyl acceptors, as well as between the dianisylamino donor with the seven-membered ring as the acceptor. This CT band is more intense but at higher energy for **1** than for **2**. Surprisingly, neither the CT band in **1** nor that in **2** shows any systematic solvatochromism in solvents ranging in polarity from MeCN to Et_2O. Because of the two-dimensional topology of the azulene derivatives it might be possible that the CT band in **1** actually consists of two perpendicularly polarised bands, although such bands are usually more strongly separated in energy.[60, 61] For derivative **2** there is a very weak shoulder at $\approx$600 nm, which might be due to the same transition that causes the blue colour of unsubstituted azulene. Azulene substituted with a dialkylamino group in the 6-position also has a CT band at about 470–500 nm, but this band shows a negative solvatochromism and is two orders of magnitude weaker ($\varepsilon \approx 1000\,\text{M}^{-1}\text{cm}^{-1}$) than the one observed in our cases.[62, 63] Azulene substituted with amino groups in the 2- and 6-positions and by ethylcarboxylate groups in the 1- and 3-positions has a somewhat stronger band ($\varepsilon \approx 5000\,\text{M}^{-1}\text{cm}^{-1}$) at the same wavelength.[64] This comparison demonstrates the very unusual linear optical absorption features of **1** and of **2** induced by the substitution pattern.

Despite the lack of solvatochromism of the CT band, **1** possesses a high ground state dipole moment, which was measured by the Hedestrand method[65] which yields $\mu_{\text{exptl}} = 7.5 \pm 0.5$ D in benzene. This value is in good agreement with the calculated (AM1) dipole moment of 8.8 D, while the AM1 value for **2** is only 2.1 D.[66] It is to some extent surprising that the CT band in **1** is at higher energy than that of **2** despite **1** having the stronger acceptor (nitrophenyl) substituents. The dipolar character of the ground and excited states or, more exactly, the changes of dipolar character can also be demonstrated by measurement of the absolute value of the first hyperpolarisability β by nonresonant HRS at 1500 nm. According to Equation (1) the hyperpolarisability of one-dimensional chromophores is only significant if the dipolar character between ground and excited states changes strongly. Indeed, HRS measurements in $CHCl_3$ solutions, in which neither **1** nor **2** shows fluorescence, yielded significant hyperpolarisabilities.[67–69] Because the nature of the electronic transitions appears to be very complicated we cannot safely assume purely one-dimensional CT behaviour. It might well be possible that octupolar contributions add to the β tensor.[16, 18, 19] Thus, evaluation of the measured HRS signals in terms of specific tensor element contributions to the β tensor is impossible, so we only give the mean $\sqrt{\langle\beta^2_{\text{HRS}}\rangle}$ values at 1500 nm: 32×10^{-30} esu for **1** and 24×10^{-30} esu for **2** (the $\beta^{\text{B}*}$ convention of Willets et al.[70] was adopted). For comparison, the mean $\sqrt{\langle\beta^2_{\text{HRS}}\rangle}$ value of disperse red DR1, which has a very similar absorption maximum ($\lambda_{\max} = 472$ nm in $CHCl_3$) is 31×10^{-30} esu under the same experimental conditions.[69, 71, 72] In this way, both azulene derivatives are quite similar to DR1 but of course they have a much higher mass.

Electron-transfer properties: Cyclic voltammetry (CV) in CH_2Cl_2/0.2 M tetrabutylammonium hexafluorophosphate (TBAH) solution indicated two reversible oxidation processes for **1** and four reversible oxidation processes for **2** (see Figure 4). The redox potentials associated with these oxidations were evaluated by digital simulation of the CVs and are given in Table 4. The redox potentials were also determined by differential pulse voltammetry.

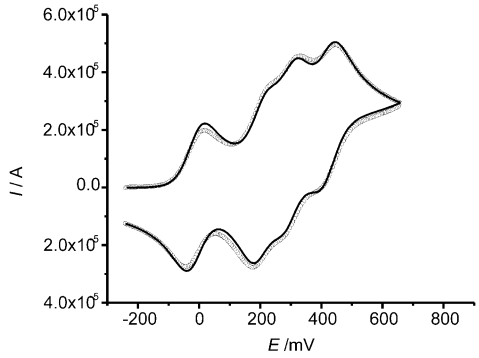

Figure 4. Cyclic voltammogram of **2** vs. ferrocene/ferrocenium at 250 mV s^{-1} in CH_2Cl_2/0.2 M TBAH at RT. Open circles: experimental data, solid line: simulation (see text for details).

Table 4. Redox potentials vs. ferrocene/ferrocenium from cyclic voltammetry at 250 mV s^{-1} in CH_2Cl_2/0.2 M TBAH at RT.

	$E_{1/2}$ [**M/M**$^+$] [mV]	$E_{1/2}$ [**M**$^+$**/M**$^{2+}$] [mV]	$E_{1/2}$ [**M**$^{2+}$**/M**$^{3+}$] [mV]	$E_{1/2}$ [**M**$^{3+}$**/M**$^{4+}$] [mV]
1	190	455		
2	−23	190	290	410

For azulene **1** we assume that the first oxidation process refers to the triarylamine at N2, which should be easily oxidisable because of the electron-donating effect of the five-membered ring of azulene. The second redox process is associated with the triarylamine around N4, because the seven-membered ring of azulene is electron-deficient. Owing to the four triarylamine redox centres and the overall associated higher electron density, the first two redox processes in **2** occur at significantly lower potential than in **1**. Because of the very complex electronic nature of **2** we refrain from assigning any of the four redox processes to a specific triarylamine group or to the azulene itself.

The UV/Vis/NIR spectroscopic properties of the radical cations of **1** and **2** were examined with the aid of a spectroelectrochemical cell,[73] in which a solution of **1** or **2** in CH_2Cl_2/0.2 M TBAH can be oxidised step by step in a thin-layer (100 μm) by application of an electrical potential to a gold mini-grid working electrode while the spectra are recorded in transmission.

Upon stepwise oxidation of **1** a strong and broad absorption at 7420 cm^{-1} (see Figure 6) appears, vanishing once again for the fully oxidised compound **1**$^{2+}$. This broad band is assigned to an intervalence charge-transfer band (IV-CT) of **1**$^+$ associated with the optically induced transfer of a hole from the triarylamine radical cation centred at N2 to the triarylamine at N4 (see also Figure 1). This band is slightly

asymmetric, as also observed in many other cases.[34] The IV-CT band, which is almost base line separated from adjacent bands, was deconvoluted by Gaussian functions[34] and integrated in order to obtain the transition moment associated with this excitation. For the evaluation of the electronic coupling V according to Equation (3) the diabatic dipole moment difference was approximated by the geometric N–N distance[34] (12.4 Å, estimated by an AM1 optimisation),[51] which then yields $V = 1140\ cm^{-1}$ (see Table 5). This coupling equals that in tetraanisyltolandiamine, **TATD**$^+$ ($V =$ 1200 cm^{-1}, $\lambda = 6190\ cm^{-1}$),[34] which is reasonable as both **1** and **TATD** have the same number of bonds (11) separating the nitrogen centres. Unfortunately, we cannot determine the reorganisation energy λ associated with the ET because the optical transition energy consists of λ *and* of the free energy difference ΔG^0, the magnitude of which is unknown. If we assume that the reorganisation energy is the same in **1**$^+$ and in **TATD**$^+$ under the same experimental conditions we can estimate ΔG^0 to be $\approx 1200\ cm^{-1}$. This free energy difference is induced by the azulene moiety itself.

Table 5. Optical parameters of the IV-CT bands in CH_2Cl_2/0.2 M TBAH at RT.

	$\tilde{\nu}_{opt}$ [cm^{-1}]	ε [$M^{-1}cm^{-1}$]	μ_{eg}[D][a]	V [cm^{-1}]
1$^+$	7420 ± 150	16500 ± 500	9.2 ± 0.5	1140 ± 60
2$^+$	6900 ± 150	14400 ± 500		
2^{2+}	6500 ± 150	12000 ± 500		
2^{3+}	5920 ± 150	23500 ± 500		

[a] For band integration we deconvoluted the spectra by use of Gaussian curves.

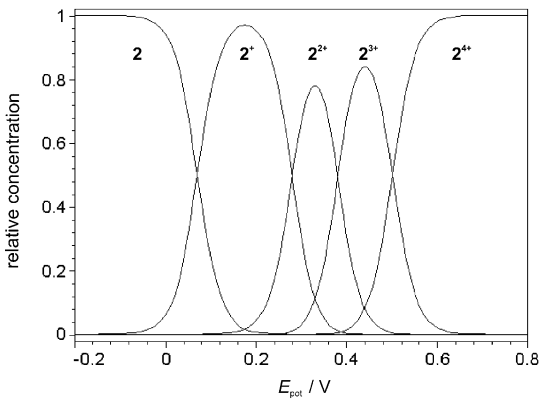

Figure 5. Relative concentrations of all redox active species **2**$^{n+}$ depending on the applied electrical potential.

The absorption bands in the NIR were therefore corrected by the following method: the spectrum of **2**$^{3+}$ at its highest absorptivity contains 8 % of the spectrum of **2**$^{2+}$ and **2**$^{4+}$. The (uncorrected) spectra of the last two cations were therefore multiplied by 0.08 and subtracted from the uncorrected spectrum of **2**$^{3+}$. The new spectrum of **2**$^{3+}$ is divided by 0.84 in order to correct the overall molar absorptivity. The same procedure was applied to the raw spectra of **2**$^+$ and **2**$^{2+}$ by using the now corrected spectrum of **2**$^{3+}$. All corrected spectra of the radical cations are given in Figure 6.

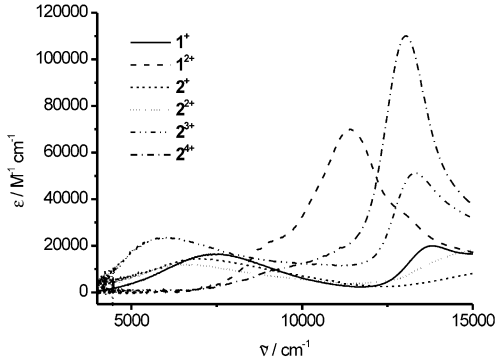

Figure 6. NIR spectra of the radical cations in CH_2Cl_2/0.2 M TBAH at RT.

The band maxima at energies above 10000 cm^{-1} are triarylamine radical cation $\pi-\pi^*$ excitations[74–76] while those below 8000 cm^{-1} are IV-CT bands. For **1**$^{2+}$ and **2**$^{4+}$ only shoulders around 10000 cm^{-1} are observed, which might be due to IV-CT excitations into the azulene bridge.[33] Because of the multidimensional nature of **2** the IV-CT bands of **2**$^+$, **2**$^{2+}$ and **2**$^{3+}$ actually consist of many sub-bands. Unlike the cases in which the high symmetry of multidimensional MV compounds[40, 41] allows the deconvolution of the IV-CT bands, this is impossible here, so we have to stay with the conclusion that the IV-CT bands of **2**$^+$ and **2**$^{2+}$ are of energy and intensity similar to that of **1**$^+$ whereas that of **2**$^{3+}$ is at much lower energy.

Conclusion

Two highly substituted azulene derivatives, the structures as well as the optical and electron transfer properties of which have been investigated in detail, were synthesised by Pd-mediated dimerisation.

Although the substitution patterns in the two azulene derivatives are quite different—four donor substituents in the 1-, 2-, 3- and 6-positions in **2** and two donors and two acceptors alternating in the 1-, 2-, 3- and 6-positions in **1**—they show the same strong bond length alternation in the crystalline state.

In comparison with the usually weak azulene band, each of these azulene derivatives has an unusually intense CT band around 450–500 nm. While this CT band shows no systematic solvatochromism, the ground-state dipole moment is significant, as are the changes to the excited-state dipole moment, as was demonstrated by HRS measurements of the first-order hyperpolarisability. The measured hyperpolarisability of **1**

and of **2** is about that of disperse red DR1, which has a similar longest-wavelength absorption.

Both azulene derivatives show multiple oxidation processes. For **2** these processes cover a broad range of ≈ 600 mV, which makes **2** an electron sponge that might be useful as a mediator in electron-transfer catalysis.[77] The intramolecular adiabatic ET behaviour of the mixed valence radical cations of **1** and of **2** was investigated by UV/Vis/NIR spectroelectrochemistry. All mixed-valence radical cations show intense IV-CT bands in the NIR. The IV-CT band of $\mathbf{1}^+$ could be analysed by the Generalised Mulliken–Hush theory, which yields an electronic coupling $V = 1140\ cm^{-1}$ for the optically induced adiabatic hole transfer. This coupling is very similar to that of dianisylamino substituted tolan **TATD**$^+$, which has the same geometric N–N distance. The free energy difference induced by the azulene moiety itself was estimated to be about $1200\ cm^{-1}$. The mixed valence states of **2** show very complex IV-CT bands, and a further detailed analysis was impossible.

In conclusion, the azulene derivatives **1** and **2** each possess both a significant ground state polarisation as well as first-order hyperpolarisability and interesting electron-transfer behaviour. This unique combination of features might be useful for the development of photorefractive materials. Chromophores with both ET and NLO properties have already been implemented quite successfully in low-glass temperature photorefractive glasses.[78] The obvious drawback of the azulene derivatives **1** and **2** is their crystallinity, which might be suppressed by incorporation of alkyl chains attached to the triarylamine groups instead of the methoxy groups. Studies in this direction, as well as concerning the excited state dynamics, are in progress.

Experimental Section

X-ray crystallography: Crystals of **1**·EtOAc were grown from a saturated benzene/ethyl acetate solution over undissolved material in a sealed glass tube by application of a temperature gradient of 45 to $\approx 30\,^\circ C$.

Crystals of **2**·MeCN were grown by slow evaporation of a benzene/$CHCl_3$ mixture at RT. Traces of MeCN from previous crystallisation attempts were present.

Both structures were solved by direct methods (SHELXS97), the hydrogen atoms being refined in idealised positions with isotropic displacement parameters. For further details see Table 1.

CCDC-197244 and -205525 contain the supplementary crystallographic data for this paper. These data can be obtained free of charge at www.ccdc.cam.ac.uk/conts/retrieving.html [or from the Cambridge Crystallographic Data Centre, 12, Union Road, Cambridge CB2 1EZ, UK; fax: (+44) 1223-336-033; E-mail: deposit@ccdc.cam.ac.uk].

Cyclic voltammetry and spectroelectrochemistry: The electrochemical experiments were performed by use of a conventional three-electrode set-up with a platinum disk working electrode in dry, nitrogen-saturated CH_2Cl_2 with 0.2 M tetrabutylammonium hexafluorophosphate (TBAH) as supporting electrolyte and 0.001 M substrate. The potentials are referenced against ferrocene (Fc/Fc^+). Digital fits of the experimental CVs were done with DigiSim[79] with the assumption of chemical and electrochemical reversibility of all processes. For spectroelectrochemical analysis, the solution of the CV experiments were transferred into a thin-layer cell[73] made up of two quartz windows with a gold mini-grid working electrode squeezed in-between. The optical path length was 100 μm. The cell design has been described elsewhere.[73] The UV/Vis/NIR spectra were recorded with a JASCO V570 spectrometer in transmission.

Hyper-Rayleigh scattering measurements: The experimental set-up and the data evaluation is described in detail in[67–69]. The 1500 nm output of an optical parametric power oscillator (OPPO) was used as the incident light. This long wavelength was chosen so as to avoid two- or three-photon induced fluorescence contributions to the HRS signal. In addition, the spectral purity of the detected signal was checked by use of different filters. All measurements were done in $CHCl_3$. The reference compound was *p*-dimethyaminocinnamaldehyde ($\beta_{zzz} = 35 \times 10^{-30}$ esu at 1500 nm in $CHCl_3$)[80] under identical experimental conditions. The accuracy of all measurements was estimated to be about ±15%. The β^{B*} convention of Willets et al.[70] has been used throughout this paper.

1,3-Bis-(4-nitrophenyl)-2-{4-[*N,N*-bis(4-methoxyphenyl)amino]phenyl}-6-[*N,N*-bis(4-methoxyphenyl)amino]azulene (1): 4-Dianisylamino-4′-nitrotolan (198 mg, 0.44 mmol) and $[Pd(PhCN)_2Cl_2]$ (100 mg, 0.260 mmol) were dissolved in dry THF (5 mL) and heated at reflux for 12 h. The solvent was removed in vacuo and the residue was purified by several flash chromatography runs (silica gel, gradient PE/CH_2Cl_2 4:1 → PE/CH_2Cl_2 1:1 → PE/CH_2Cl_2 1:3) followed by precipitation from CH_2Cl_2/PE to yield a red solid (40 mg, 0.044 mmol, 20%). M.p. 226 °C; ^{1}H NMR (400 MHz, $CDCl_3$): $\delta =$ 8.16, 7.39 (AA′, 4H; H-3′ and BB′, 4H; H-2′ nitrophenyl), 7.91, 6.80 (AA′, 2H; H-4, and BB′, 2H; H-5, azulene), 7.16, 6.79 (AA′, 4H; H-8 and BB′, 4H; H-9, methoxyphenyl), 7.03–6.89 (AA′-BB′, 8H; H-6″, H-7″, methoxyphenyl), 6.67–6.64 (AA′-BB′, 4H; H-2″ and H-3″, aminophenyl), 3.81 (s, 6H; methoxy), 3.77 (s, 6H; methoxy); ^{13}C NMR (101 MHz, $CDCl_3$): $\delta =$ 159.1, 157.8, 156.0, 147.5, 145.7, 144.3, 142.6, 140.4, 139.0, 134.3, 132.3, 131.8, 131.7, 119.1, 128.2, 127.2, 126.9, 126.9, 123.2, 117.2, 115.3, 114.7, 55.52, 55.46; FAB-MS (high resolution, PI): calcd for $C_{56}H_{44}N_4O_8$: 900.3159; found: 900.31798; $\Delta = 2.3$ ppm.

1,2,3-Tris-{4-[*N,N*-bis(4-methoxyphenyl)amino]phenyl}-6-[*N,N*-bis(4-methoxyphenyl)-amino]azulene (2): 4,4′-Tetraanisyltolandiamine **TADT** (100 mg, 0.16 mmol) and $[Pd(PhCN)_2Cl_2]$ (37 mg, 0.097 mmol) were dissolved in dry THF (5 mL) and heated at reflux for 12 h. The solvent was removed in vacuo and the residue was purified by flash chromatography (alumina, neutral +7% H_2O, CH_2Cl_2) followed by precipitation from CH_2Cl_2/MeOH to yield a red solid (30 mg, 0.024 mmol, 30%). M.p. 140 °C; ^{1}H NMR (400 MHz, [D$_8$]THF): $\delta = 7.82$ (AA′, 2H; H-4, azulene), 7.13 (AA′, 4H), 7.05–6.75 (AA′- and BB′overlapping, 38H), 6.66 (BB′, 2H; aminophenyl), 6.59 (BB′, 2H; H-5, azulene), 3.77 (s, 6H; methoxy), 3.74 (s, 6H; methoxy), 3.74 (s, 12H; methoxy); ^{13}C NMR (101 MHz, [D$_8$]THF): $\delta =$ 158.6, 158.3, 156.9, 156.8, 147.5, 147.4, 143.2, 142.0, 141.8, 140.9, 134.5, 133.3, 130.5, 130.5, 130.2, 132.6, 132.5, 128.7, 127.2, 127.0, 121.0, 119.9, 116.3, 115.6, 115.2, 115.2, 55.5, 55.4, 55.4. EI-MS (high resolution, PI): calcd for $C_{84}H_{72}N_4O_8$: 1264.5350; found: 1264.53840; $\Delta = 2.4$ ppm.

Acknowledgements

This work was supported by the Fonds der Chemischen Industrie, the Deutsche Forschungsgemeinschaft (Graduiertenkolleg "Elektronendichte") and the Bayerisches Staatsministerium für Wissenschaft, Forschung und Kunst (FORMAT project). We thank Prof. J. Daub, Regensburg, H. Poepke, Regensburg and JASCO GmbH Deutschland for kind support.

[1] F. X. Redl, O. Köthe, K. Röckl, W. Bauer, J. Daub, *Macromol. Chem. Phys.* **2000**, *201*, 2091.
[2] M. Porsch, G. Sigl-Seifert, J. Daub, *Adv. Mater.* **1997**, *9*, 635.
[3] S. Schmitt, M. Baumgarten, J. Simon, K. Hafner, *Angew. Chem.* **1998**, *110*, 1129; *Angew. Chem. Int. Ed.* **1998**, *37*, 1077.
[4] T. Mrozek, H. Görner, J. Daub, *Chem. Eur. J.* **2001**, *7*, 1028.
[5] G. Iftime, P. G. Lacroix, K. Nakatani, A. C. Razus, *Tetrahedron Lett.* **1998**, *39*, 6853.
[6] R. Herrmann, B. Pedersen, G. Wagner, J.-H. Youn, *J. Organomet. Chem.* **1998**, *571*, 261.
[7] T. Farrell, T. Meyer-Friedrichsen, M. Malessa, D. Haase, W. Saak, I. Asselberghs, K. Wostyn, K. Clays, A. Persoons, J. Heck, A. R. Manning, *J. Chem. Soc. Dalton Trans.* **2001**, 29.
[8] A. E. Asato, R. S. H. Liu, V. P. Rao, Y. M. Cai, *Tetrahedron Lett.* **1996**, *37*, 419.

[9] P. Wang, P. Zhu, C. Ye, A. E. Asato, R. S. H. Liu, *J. Phys. Chem. A* **1999**, *103*, 7076.
[10] J. N. Woodford, C. H. Wang, A. E. Asato, R. S. H. Liu, *J. Chem. Phys.* **1999**, *111*, 4621.
[11] P. G. Lacroix, I. Malfant, G. Iftime, A. C. Razus, K. Nakatani, J. A. Delaire, *Chem. Eur. J.* **2000**, *6*, 2599.
[12] E. Hendrickx, K. Clays, A. Persoons, *Acc. Chem. Res.* **1998**, *31*, 675.
[13] B. S. Brunschwig, C. Creutz, N. Sutin, *Chem. Soc. Rev.* **2002**, *31*, 168.
[14] J.-P. Launay, *Chem. Soc. Rev.* **2001**, *30*, 386.
[15] J. J. Wolff, R. Wortmann, *Adv. Phys. Org. Chem.* **1999**, *32*, 121.
[16] T. Verbiest, S. Houbrechts, M. Kauranen, K. Clays, A. Persoons, *J. Mater. Chem.* **1997**, *7*, 2175.
[17] J. L. Oudar, D. S. Chemla, *J. Chem. Phys.* **1977**, *66*, 2664.
[18] J. J. Wolff, R. Wortmann, *J. Prakt. Chem.* **1998**, *340*, 99.
[19] J. Zyss, I. Ledoux, *Chem. Rev.* **1994**, *94*, 77.
[20] M. Joffre, D. Yaron, R. J. Silbey, J. Zyss, *J. Chem. Phys.* **1992**, *97*, 5607.
[21] C. Lambert, E. Schmälzlin, K. Meerholz, C. Bräuchle, *Chem. Eur. J.* **1998**, *4*, 512.
[22] C. Lambert, W. Gaschler, E. Schmälzlin, K. Meerholz, C. Bräuchle, *J. Chem. Soc. Perkin Trans. 2* **1999**, 577.
[23] K. D. Demadis, C. M. Hartshorn, T. J. Meyer, *Chem. Rev.* **2001**, *101*, 2655.
[24] C. Creutz, *Progr. Inorg. Chem.* **1983**, *30*, 1.
[25] R. J. Crutchley, *Adv. Inorg. Chem.* **1994**, *41*, 273.
[26] S. F. Nelsen, R. F. Ismagilov, D. A. Trieber, *Science* **1997**, *278*, 846.
[27] S. F. Nelsen, *Chem. Eur. J.* **2000**, *6*, 581.
[28] T. H. Jozefiak, J. E. Almlof, M. W. Feyereisen, L. L. Miller, *J. Am. Chem. Soc.* **1989**, *111*, 4105.
[29] S. F. Rak, L. L. Miller, *J. Am. Chem. Soc.* **1992**, *114*, 1388.
[30] M. Mayor, M. Büschel, K. M. Fromm, J.-M. Lehn, J. Daub, *Chem. Eur. J.* **2001**, *7*, 1266.
[31] J. Bonvoisin, J.-P. Launay, M. Van der Auweraer, F. C. De Schryver, *J. Phys. Chem.* **1994**, *98*, 5052.
[32] J. Bonvoisin, J.-P. Launay, W. Verbouwe, M. Van der Auweraer, F. C. De Schryver, *J. Phys. Chem.* **1996**, *100*, 17079.
[33] C. Lambert, G. Nöll, J. Schelter, *Nat. Mater.* **2002**, *1*, 69.
[34] C. Lambert, G. Nöll, *J. Am. Chem. Soc.* **1999**, *121*, 8434.
[35] C. Lambert, G. Nöll, *Angew. Chem.* **1998**, *110*, 2239; *Angew. Chem. Int. Ed.* **1998**, *37*, 2107.
[36] P. Strohriegl, J. V. Grazulevicius, *Adv. Mater.* **2002**, *14*, 1439.
[37] D. P. West, M. D. Rahn, in *Electron Transfer in Chemistry*, *Vol. 5* (Ed.: V. Balzani), Wiley-VCH, Weinheim, **2001**, pp. 472.
[38] M. Grätzel, J.-E. Moser, in *Electron Transfer in Chemistry*, *Vol. 5* (Ed.: V. Balzani), Wiley-VCH, Weinheim, **2001**, pp. 589.
[39] J. C. Scott, G. G. Malliaras, in *Semiconducting Polymers* (Eds.: G. Hadziioannou, P. v. Hutten), Wiley-VCH, Weinheim, **2000**, pp. 411.
[40] C. Lambert, G. Nöll, F. Hampel, *J. Phys. Chem. A* **2001**, *105*, 7751.
[41] C. Lambert, G. Nöll, *Chem. Eur. J.* **2002**, *8*, 3467.
[42] C. Lambert, G. Nöll, *Synth. Met.* **2003**, in press.
[43] M. D. Newton, *Chem. Rev.* **1991**, *91*, 767.
[44] M. D. Newton, *Adv. Chem. Phys.* **1999**, *106*, 303.
[45] C. Creutz, M. D. Newton, N. Sutin, *J. Photochem. Photobiol. A: Chem.* **1994**, *82*, 47.
[46] N. S. Hush, *Coord. Chem. Rev.* **1985**, *64*, 135.
[47] J. P. Chang, E. Y. Fung, J. C. Curtis, *Inorg. Chem.* **1986**, *25*, 4233.
[48] Y. J. Chen, C.-H. Kao, S. J. Lin, C.-C. Tai, K. S. Kwan, *Inorg. Chem.* **2000**, *39*, 189.
[49] C. Lambert, G. Nöll, *J. Chem. Soc. Perkin Trans. 2* **2002**, 2039.
[50] R. J. Cave, M. D. Newton, *Chem. Phys. Lett.* **1996**, *249*, 15.
[51] Taking $e \times r$ as an estimate for the diabatic dipole moment difference might be a strong overestimation. Recent studies on bis(triarylamine) radical cations indeed show that the diabatic dipole moment is much smaller, see ref. [81, 82]. A smaller dipole moment difference would result in a higher electronic coupling in $\mathbf{1}^+$ and $\mathbf{TD}^+$ but would leave all other conclusions unchanged.
[52] C. Lambert, *ChemPhysChem* **2003**, *4*, 877.
[53] E. Müller, G. Zountsas, *Chem. Ztg.* **1973**, *97*, 447.
[54] E. Müller, G. Zountsas, *Chem. Ztg.* **1974**, *98*, 41.
[55] C. J. Cooksey, J. L. Courtneidge, A. G. Davies, P. S. Gregory, J. C. Evans, C. C. Rowlands, *J. Chem. Soc. Perkin Trans. 2* **1988**, 807.
[56] J. M. Robertson, H. M. M. Shearer, G. A. Sim, D. G. Watson, *Acta Crystallogr.* **1962**, *15*, 1.
[57] M. J. Bearpark, F. Bernardi, S. Clifford, M. Olivucci, M. A. Robb, B. R. Smith, T. Vreven, *J. Am. Chem. Soc.* **1996**, *118*, 169.
[58] Y. Lu, D. M. Lemal, J. P. Jasinski, *J. Am. Chem. Soc.* **2000**, *122*, 2440.
[59] A. W. Hanson, *Acta Crystallogr.* **1965**, *19*, 19.
[60] R. Wortmann, P. Krämer, C. Glania, S. Lebus, N. Detzer, *Chem. Phys.* **1993**, *173*, 99.
[61] J. J. Wolff, D. Längle, D. Hillenbrand, R. Wortmann, R. Matschiner, C. Glania, P. Krämer, *Adv. Mater.* **1997**, *9*, 138.
[62] H. G. Löhr, F. Vögtle, *Chem. Ber.* **1985**, *118*, 905.
[63] J. Zindel, S. Maitra, D. A. Lightner, *Synthesis* **1996**, 1217.
[64] T. Nozoe, K. Takase, M. Tada, *Bull. Chem. Soc. Jpn.* **1963**, *36*, 1006.
[65] O. Exner, *Dipole Moments in Organic Chemistry*, Thieme, Stuttgart, **1975**.
[66] J. J. P. Stewart, *MOPAC97*, Fujitsu Limited, **1997**.
[67] S. Stadler, G. Bourhill, C. Bräuchle, *J. Phys. Chem.* **1996**, *100*, 6927.
[68] S. Stadler, R. Dietrich, G. Bourhill, C. Bräuchle, *Opt. Lett.* **1996**, *21*, 251.
[69] S. Stadler, R. Dietrich, G. Bourhill, C. Bräuchle, A. Pawlik, W. Grahn, *Chem. Phys.* **1995**, *247*, 271.
[70] A. Willetts, J. E. Rice, D. M. Burland, D. P. Shelton, *J. Chem. Phys.* **1992**, *97*, 7590.
[71] C. Lambert, G. Nöll, E. Schmälzlin, K. Meerholz, C. Bräuchle, *Chem. Eur. J.* **1998**, *4*, 2129.
[72] We stress that **1** and **2** as possible two-dimensional chromophores cannot be safely referenced against DR1 as a one-dimensional chromophore because polarisation conditions were not taken into account in our measurements, see ref. [83].
[73] J. Salbeck, *Anal. Chem.* **1993**, *65*, 2169.
[74] F. A. Neugebauer, S. Bamberger, W. R. Groh, *Chem. Ber.* **1975**, *108*, 2406.
[75] W. Schmidt, E. Steckhan, *Chem. Ber.* **1980**, *113*, 577.
[76] S. Dapperheld, E. Steckhan, K.-H. G. Brinkhaus, T. Esch, *Chem. Ber.* **1991**, *124*, 2557.
[77] E. Steckhan, *Angew. Chem.* **1986**, *98*, 681; *Angew. Chem. Int. Ed.* **1986**, *25*, 693.
[78] F. Würthner, R. Wortmann, K. Meerholz, *ChemPhysChem* **2002**, *3*, 17.
[79] M. Rudolph, S. W. Feldberg, *DigiSim 3.03a*, Bioanalytical Systems, Inc., West Lafayette, IN (USA), **1994–2000**.
[80] E. Schmälzlin, K. Meerholz, S. Stadler, C. Bräuchle, H. Patzelt, D. Oesterhelt, *Chem. Phys. Lett.* **1993**, *280*, 551.
[81] S. F. Nelsen, A. E. Konradsson, Y. Luo, K.-Y. Kim, S. C. Blackstock, unpublished results.
[82] V. Coropceanu, C. Lambert, G. Nöll, J.-L. Brédas, *Chem. Phys. Lett.* **2003**, *373*, 153.
[83] P. Kaatz, D. P. Shelton, *J. Chem. Phys.* **1996**, *105*, 3981.

Received: March 7, 2003 [F4923]

